

Citation for published version:

Mellon, SJ, Grammatopoulos, G, Andersen, M, Pandit, H, Gill, HS & Murray, D 2015, 'Optimal acetabular component orientation estimated using edge-loading and impingement risk in patients with metal-on-metal hip resurfacing arthroplasty', *Journal of Biomechanics*, vol. 48, no. 2, pp. 318-23.
<https://doi.org/10.1016/j.jbiomech.2014.11.027>

DOI:

[10.1016/j.jbiomech.2014.11.027](https://doi.org/10.1016/j.jbiomech.2014.11.027)

Publication date:

2015

Document Version

Early version, also known as pre-print

[Link to publication](#)

University of Bath

Alternative formats

If you require this document in an alternative format, please contact:
openaccess@bath.ac.uk

General rights

Copyright and moral rights for the publications made accessible in the public portal are retained by the authors and/or other copyright owners and it is a condition of accessing publications that users recognise and abide by the legal requirements associated with these rights.

Take down policy

If you believe that this document breaches copyright please contact us providing details, and we will remove access to the work immediately and investigate your claim.

**Optimal acetabular component orientation estimated using edge-loading and
impingement risk in patients with metal-on-metal hip resurfacing arthroplasty**

Stephen J. Mellon¹, George Grammatopoulos¹, Michael S. Andersen², Hemant G. Pandit¹,
Harinderjit S. Gill^{1,3} and David W. Murray¹

1. Nuffield Department of Orthopaedics, Rheumatology and Musculoskeletal Sciences,
University of Oxford, United Kingdom

2. Department of Mechanical and Manufacturing Engineering, Aalborg University,
Denmark

3. Department of Mechanical Engineering, University of Bath, United Kingdom

Original Article

Word Count: 2970

stephen.mellon@ndorms.ox.ac.uk

Nuffield Department of Orthopaedics, Rheumatology and Musculoskeletal Sciences

University of Oxford,

Nuffield Orthopaedic Centre,

Windmill Road,

OXFORD,

OX3 7LD

+44 (0)1865 227454

Keywords: Hip, Metal-on-Metal, Impingement, Edge-loading, Kinematics,

Abstract

Edge-loading in patients with metal-on-metal resurfaced hips can cause high serum metal ion levels, the development of soft-tissue reactions local to the joint called pseudotumours and ultimately, failure of the implant. Primary edge-loading is where contact between the femoral and acetabular components occurs at the edge/rim of the acetabular component whereas impingement of the femoral neck on the acetabular component's edge causes secondary or contrecoup edge-loading. While the relationship between the orientation of the acetabular component and primary edge-loading has been identified, the contribution of acetabular component orientation to impingement and secondary edge-loading is less clear. Our aim was to estimate the optimal acetabular component orientation for 16 metal-on-metal hip resurfacing arthroplasty (MoMHRA) subjects with known serum metal ion levels. Data from motion analysis, subject-specific musculoskeletal modelling and Computed Tomography (CT) measurements were used to calculate the dynamic contact patch to rim (CPR) distance and impingement risk for 3416 different acetabular component orientations during gait, sit-to-stand, stair descent and static standing. For each subject, safe zones free from impingement and edge-loading (CPR <10%) were defined and, consequently, an optimal acetabular component orientation was determined (mean inclination 39.7° (SD 6.6°) mean anteversion 14.9° (SD 9.0°)). The results of this study suggest that the optimal acetabular component orientation can be determined from a patient's motion and anatomy. However, 'safe' zones of acetabular component orientation associated with reduced risk of dislocation and pseudotumour are also associated with a reduced risk of edge-loading and impingement.

Introduction

Metal-on-metal hip resurfacing arthroplasty (MoMHRA) became an established surgical option in the late 1990s/early 2000s, particularly for the young active patient with end-stage hip disease. In England and Wales in 2006, 10% of all primary total hip replacements performed were MoMHRA. However, subsequent concerns about high revision rates and soft tissue reactions meant that by 2012 usage had fallen to 1%.

Occurrence of soft tissue or fluidic masses local to the hip joint (pseudotumour (Pandit et al., 2008a), adverse reaction to metal debris (Langton et al., 2010)), aseptic lymphocytic vasculitis associated lesions (Willert et al., 2005), adverse local tissue reaction (Schmalzried, 2009)) are associated with high blood, serum and hip aspirate levels of cobalt (Co) and chromium (Cr); the principal elements of the metal alloy used to manufacture MoMHRA implants (De Smet et al., 2008a; Kwon et al., 2009; Langton et al., 2009a). This indicates these reactions are associated with increased levels of wear. Retrieval studies have confirmed that implants revised for pseudotumour have higher wear than implants revised for other reasons (Kwon et al., 2010). Retrieval studies have also shown that implants revised for pseudotumour are more likely to have experienced edge-loading (Kwon et al., 2010; Langton et al., 2011).

Primary edge-loading is the result of contact between the femoral and acetabular components at the edge of the acetabular component while contact between the femoral neck and the cup edge causes secondary or countercoup edge-loading. The occurrence of primary edge-loading has shown an association with acetabular component orientation (De Haan et al., 2008b). The risk of pseudotumour is reduced for an acetabular component orientation of 45° ($\pm 10^\circ$) inclination and 20° ($\pm 10^\circ$) anteversion (Grammatopoulos et al., 2011). This relationship

between acetabular component orientation and risk of edge-loading has been further highlighted by studies that have calculated the distance of the hip contact force vector from the edge of the acetabular component (contact patch to rim distance). This has been carried out using two methods: by using the average hip contact force (HCF) vector of four subjects with instrumented prostheses standing (Bergmann et al., 2001) and calculating the 3D position of the acetabular component from Computed Tomography (CT) scans or radiographs (Langton et al., 2009b; Matthies et al., 2014; Yoon et al., 2013) or by carrying out motion analysis and CT scans of subjects and musculoskeletal modelling to define the HCF vector for activities of daily living (Mellon et al., 2013).

The contribution of secondary edge-loading (impingement) to wear of metal-on-metal hip resurfacing arthroplasty (MoMHRA) is more difficult to determine and consequently fewer studies have investigated this. Radiographic signs of impingement have been shown to have an association with elevated serum ion levels of cobalt and chromium but only in combination with poor acetabular component orientation (Le Duff et al., 2014).

The relationship between component positioning and the occurrence of high metal ion levels and/or pseudotumours is not clear-cut. Subjects with “well-placed” components have developed pseudotumours, albeit in small numbers (Donell et al., 2010; Grammatopoulos et al., 2011; Kwon et al., 2011; Matthies et al., 2012) and some patients with mal-positioned components avoid high metal ion levels (Grammatopoulos et al., 2011; Matthies et al., 2012). The reasons for this are unclear although it has been suggested that high wear and/or the occurrence of pseudotumours are associated with other factors such as implant design, metal hypersensitivity (Pandit et al., 2008b), or an individual’s motion patterns (Mellon et al., 2013).

The aim of this study was to identify the optimal acetabular component orientation for a group of MoMHRA patients based on primary edge-loading and impingement (secondary edge-loading) risk calculated dynamically for four activities of daily living.

Method: Patients

In an on-going study, a cohort of 158 (201 hips) MoMHRA patients have their serum metal ion levels measured regularly. Sixteen subjects (seven females and nine males) from this 158 with unilateral MoMHRA with metal ion levels that represented the range of the whole cohort responded to a written request and agreed to participate in the current IRB approved study. The subjects had either a Birmingham Hip Resurfacing (BHR) (Smith and Nephew, Birmingham, UK) (n=8) or a Conserve Plus (Wright Medical Technology, Memphis, TN, USA) hip resurfacing (n=8). The Laboratory of Clinical Biology, University Hospital Ghent, Belgium used inductively-coupled plasma mass spectrometry (ELAN DRC II, PerkinElmer Life and Analytical Sciences, Shelton, CT, USA) to determine the subjects' serum levels of cobalt and chromium (De Smet et al., 2008b).

Method: Motion Analysis

A laboratory equipped with 12 camera Vicon MX system (Oxford Metrics Ltd., Oxford, UK) and three force platforms (2 × OR6 AMTI R6-6-1000, 1 × OR6 AMTI R6-7-1000, Advanced Medical Technology Inc., MA, USA) was used to conduct motion analysis. An established (Kadaba et al., 1990) marker configuration with extra markers on the medial femoral condyles, the tibial tuberosities, the medial malleoli, the distal 5th and 1st metatarsals was used (25 markers total).

The subjects' motion was measured during four activities of daily living (ADL): walking, sit-to-stand, static standing and stair descent. Kinematic and force plate data were collected with a sampling rate of 100 Hz and 1000 Hz, respectively.

Method: Computed Tomography (CT) Scans

Immediately following motion analysis, retro-reflective motion analysis markers were removed and replaced with radio-opaque markers and CT scans (Siemens Somatom, Siemens Medical Solutions USA, Inc., NY, USA) of each subject's pelvis and lower limbs were obtained. The 3D coordinates of the markers, the anatomical pelvic landmarks, the MoMHRA components, the points around the femoral neck and hip joint centre were determined (SliceOmatic, V4.2, TomoVision, Virtual Magic Inc., Montreal, Canada).

Method: Musculoskeletal Modelling

Subjects were modeled performing static standing, gait, sit-to-stand and stair descent in the AnyBody Modeling System (v.5.0, AnyBody Technology A/S, Aalborg, Denmark). Each model incorporated subject-specific hip joint centres (HJC) derived from the individual CT scans, as well as nonlinear scaling methods to adapt the lower limb model to a given geometry. The musculoskeletal model used a three-stage procedure. Firstly, the patient-specific joint kinematics were estimated based on a stick-figure model constructed from the standing reference frame and the estimated HJCs. Secondly, the Twente Lower Extremity Model (TLEM) (Klein Horsman et al., 2007) implemented in the AnyBody Managed Model Repository v.1.2 was non-linearly morphed using Radial Basis Functions (RBF) (Lund, 2011) to match the segment lengths, joint parameters of the stick-figure model and subject-specific pelvis bony landmarks (ASIS and PSI) and estimated hip joint centres estimated from the CT scan. Inverse dynamic analysis was performed for the morphed TLEM model with the

measured ground reaction forces as external loads and polynomial muscle recruitment criterion of power 3 to estimate muscle and joint contact forces (Klein Horsman et al., 2007). The capsular ligaments were not included in the model.

Method: Edge-loading & Impingement Risk

Edge-loading and impingement risk was determined for all possible cup orientations, in 1° intervals, between 20° and 80° inclination and -15° and 40° anteversion (3,416 orientations). The edge-loading risk for every orientation was determined using the Contact Patch to Rim (CPR) distance. The CPR distance is the location of the intersection of the HCF with the inner surface of the acetabular component relative to the edge/rim of the component. The point of intersection is assumed to be the centre of the contact patch between the two components. All CON implants were modeled with an acetabular component with a coverage angle (α) of 170° and a diametrical clearance of 173 μm (Campbell et al., 2006). The coverage angle for the BHR acetabular component was dependent on the size of the implant and varied from 159.1° to 166.2° (Board and Walter, 2010).

The CPR distance was calculated for each subject for gait, stair descent, static standing and sit-to-stand. The analysis was limited to the periods during the dynamic activities when loads were highest i.e. stance phase during gait and stair descent and after seat-off for sit-to-stand. CPR distance was calculated as a percentage of half the inner circumference of the acetabular component to allow comparison between subjects with different sized components. At each acetabular component orientation, the lowest CPR distance out of the three ADLs was recorded.

Impingement risk was calculated for the same cup orientations examined for edge-loading risk. The 3D coordinates of points around the femoral neck on the implanted side were transformed into a coordinate system local to the femoral component (i.e. 'Z' axis parallel with the stem, origin at the HJC). The points were projected into the pelvic transverse plane and an ellipse was fitted to them (Figure 1). The 3D position of this ellipse, relative to the HJC, was determined by the size of the subject's femoral component. The position of the ellipse relative to the cup edge for each of the 4 ADLs at each orientation was calculated. If the height of the ellipse was greater than the height of the cup edge at any point during any of the ADL, then this was considered as impingement.

Contour plots for edge-loading (Figure 2(a)) and impingement risk (Figure 2(b)) were generated for each subject. These were combined and a safe zone of orientations free from impingement or edge-loading was established ($CPR < 10\%$) (Figure 2(c)). An optimum acetabular component orientation was calculated by finding the orientation where edge-loading and impingement risk was lowest. This was not simply the highest value of CPR within the safe zone as in the majority of cases, this would have occurred immediately adjacent to the impingement boundary. The risk of impingement for orientations within the safe zone was lowest for orientations furthest from the boundary. In order to factor this into the definition of optimal orientation, the distance to the boundary was calculated using Delaunay triangulation and added to the CPR distance at each orientation within the safe zone (Figure 2(d)). Within the safe zone, the orientation with the highest value was taken as the optimal orientation. The optimal orientations for all sixteen subjects were then compared to zones associated with reduced risk of dislocation (Lewinnek et al., 1978a) and pseudotumour (Grammatopoulos et al., 2010).

Method: Statistical Analysis

The change in angle required to move the subjects' actual acetabular component orientation to the optimal was calculated. The relationship of this angle with the concentration of serum chromium and cobalt ions was tested using Pearson Correlation (SPSS v20.0, IBM Inc, Chicago, USA). The R^2 correlation coefficient was also calculated.

The smallest distance from the subjects' actual acetabular component orientation to the boundary of the safe zone (implant position to boundary, IPB) was calculated (Figure 3). This value was positive when the subject's implant position occurred inside the safe zone and negative when outside. Pearson correlation was used to test the relationship between IPB and serum metal ion levels of cobalt and chromium (SPSS v20.0, IBM Inc, Chicago, USA). The R^2 correlation coefficient was also calculated for metal ions and IPB. The identification of a safe zone for each subject using edge-loading and impingement risk would be deemed valid if, for example, the acetabular component orientation of subjects with the lowest serum metal ion levels were within the safe zone with the highest values of IPB or subjects with the highest serum metal ion levels had actual implant orientations outside or close to the boundary.

Results

The optimal orientations calculated for each subject based on the orientation within their safe zone and furthest from its boundary can be seen in Table 1. The mean optimal acetabular component inclination was 39.7° (St.Dev. 6.6°) which was lower than the mean actual inclination at 51.1° (St.Dev. 9.2°). The mean optimal anteversion was 14.9° (St.Dev. 9.0°) whereas the actual anteversion was 13.9° (St.Dev. 11.1°). Four subjects' optimal orientation were outside zones associated with reduced risk of pseudotumour (Grammatopoulos et al.,

2010) or dislocation (Lewinnek et al., 1978a) (Figure 4). For the subjects' actual acetabular component orientation, both the Lewinnek and Grammatopoulos boxes contained the same number (37.5%) of subjects. For the calculated optimal acetabular component orientation, 12 (75%) of the subjects were in the Lewinnek box while 8 (50%) were in the Grammatopoulos box.

The angle from the subjects' actual acetabular component orientation to the calculated optimal orientation (Table 1) did not correlate with the concentration of serum chromium ($p > 0.05$, $R^2 = 0.02$) or serum cobalt ($p > 0.05$, $R^2 = 0.0004$).

The position of the subjects' actual acetabular component orientation relative to the safe zone boundary was calculated (IPB). There was a statistically significant correlation between the IPB and the concentration of both serum chromium ions ($p = 0.01$, $R^2 = 0.33$) and serum cobalt ions ($p = 0.016$, $R^2 = 0.29$) (Figure 5).

Discussion

In this study, we examined a group of sixteen MoMHRA subjects. The risk of edge-loading and impingement were calculated during gait, sit-to-stand, stair descent and static standing for 3,416 possible orientations of the acetabular component. A safe zone of orientations free from edge-loading and impingement was identified for each subject and consequently the optimal orientation was calculated. The results of this study suggest that zones, associated with reduced risk of dislocation or pseudotumour, are also associated with reduced risk of impingement and edge-loading.

Previous studies of acetabular component positioning have suggested that “well-positioned” acetabular components improve hip movement, minimise contact stresses and reduce the risk of impingement and/or dislocation (D'Lima et al., 2000; Del Schutte et al., 1998; Kennedy et al., 1998; Lewinnek et al., 1978b; Widmer and Zurfluh, 2004). However, a universally applicable set of evidence-based guidelines for achieving the optimal orientation for the acetabular component in total hip replacement (THR) does not exist. On the basis of radiographic analysis, Lewinnek et al., (1978b) suggested that an acetabular component orientation of 40° ($\pm 10^\circ$) inclination and 15° ($\pm 10^\circ$) anteversion, reduced the risk of dislocation. Perhaps as a result, the importance of acetabular component orientation in hip resurfacing may have been initially underestimated because of the lower dislocation risk associated with large diameter femoral components (Grammatopoulos et al., 2010; Schmalzried, 2009). However, it is now known that there is an association in patients with acetabular components with inclination angles $>55^\circ$ and elevated levels of serum metal ions (De Haan et al., 2008a; Langton et al., 2008; Langton et al., 2009b). Furthermore, an inverse relationship between component positioning, metal ion levels and static (Langton et al., 2009b; Matthies et al., 2014; Yoon et al., 2013) and dynamic (Mellon et al., 2013) hip contact forces has been identified using the CPR distance.

Impingement in previous incarnations of hip resurfacing have been reported (Chandler et al., 1982; Wiadrowski et al., 1991); In 109 retrieved Wagner metal-on-polyethylene resurfacing components, Wiadrowski et al. (1991) found evidence of eccentric wear at the rim of the acetabular component secondary to impingement of the femoral neck in 84% of cases (Beaulé et al., 2007). Several studies have identified cases of femoral neck to cup impingement at a prevalence ranging from 6% to 22% (Gruen et al., 2011; Le Duff et al., 2014; Lim et al., 2012; Yoo et al., 2011). The contribution of impingement to wear of

MoMHRA is not clear. It has been shown previously that signs of impingement, detected in radiographs, influenced serum levels of cobalt and chromium only when the functional head coverage was insufficient due to poor socket positioning. Radiographic impingement signs alone were not a good predictor of elevated metal ion levels (Le Duff et al., 2014).

The smallest distance from the boundary of the safe zone to the subjects' implant position (IPB) correlated with concentrations of both serum levels of cobalt and chromium ions. These results suggest that wear of MoMHRA for a range of acetabular component orientations can be predicted using a patient's motion and anatomy. The current study is the first to relate the effects of component positioning, component design, bony anatomy and the individual's motion patterns to implant wear. However, the inclusion of an activity that induced significant hip abduction/adduction may have improved the predictive capabilities of the model in the current study. It has been suggested that the risk of edge loading is dramatically reduced by combining deep hip flexion with hip abduction (van Arkel et al., 2013).

Our long term aim is to develop a pre-operative patient-specific method for determining optimal acetabular component orientation. In this study, which will contribute to the aim, we are limited to post-operative data. Also, ideally we would address this aim with studies on conventional (metal-on-plastic) Total Hip Arthroplasty (THA), as the majority of patients with end-stage hip osteoarthritis will receive these. However, patients with MoMHRA are a useful analogue because wear of the prosthesis is proportional to serum metal ion levels. Metal-on-Metal THA does not provide the same opportunity for study as in these patients, metal ions levels may come from the trunnion as well as the articular surface.

When simulating all the possible orientations between 20 to 80° of inclination and -15 to 40° of anteversion, the acetabular component was rotated about a fixed point, the HJC. In reality, this centre of rotation would have been different for different component orientations. Also, this model was developed under the assumption that the patient's kinematics and estimated hip contact forces would remain the same throughout all the acetabular component orientations that were analysed. The CPR calculations carried out in this study were based on the assumption that the hip contact force vector passed through the centre of a contact patch between the femoral and acetabular components. The size of this patch is determined by the force magnitude, the size/geometry/material properties of the components, the clearance between the components and the presence of lubrication. It was not possible to include this complex contact condition in our calculations of CPR.

True optimal orientation is patient-specific and can be determined with dynamic assessment, however, zones of acetabular component orientation associated with reduced risk of dislocation (Lewinnek et al., 1978a) and pseudotumour (Grammatopoulos et al., 2010) are also associated with reduced risks of impingement and edge-loading in MoMHRA.

Acknowledgements: Financial support was provided by ORUK, Depuy, McMinn Bursary (British Hip Society) and NIHR BRU.

References

- Beaulé, P.E., Harvey, N., Zaragoza, E., Le Duff, M.J., Dorey, F.J., 2007. The femoral head/neck offset and hip resurfacing. *Journal of Bone & Joint Surgery, British Volume* 89-B, 9-15.
- Bergmann, G., Deuretzbacher, G., Heller, M., Graichen, F., Rohlmann, A., Strauss, J., Duda, G.N., 2001. Hip contact forces and gait patterns from routine activities. *Journal of Biomechanics* 34, 859-871.

322 Board, T., Walter, W., 2010. When is 45 degrees not 45 degrees? Analysis of the true
323 inclination angle of resurfacing sockets. *Journal of Bone & Joint Surgery, British Volume* 92-
324 B, 397.

325 Campbell, P., Beaulé, P.E., Ebrahimpour, E., LeDuff, M., De Smet, K., Lu, Z., Amstutz, H.C.,
326 2006. The John Charnley Award: a study of implant failure in metal-on-metal surface
327 arthroplasties. *Clin Orthop Relat Res* 453, 35-46.

328 Chandler, D.R., Glousman, R., Hull, D., McGuire, P.J., Clarke, I.C., Sarimienta, A., 1982.
329 Prosthetic Hip Range of Motion and Impingement: The Effects of Head and Neck Geometry.
330 *Clin Orthop Relat Res* 166, 284-291.

331 D'Lima, D.D., Urquhart, A.G., Buehler, K.O., Walker, R.H., Colwell, C.W., 2000. The effect
332 of the orientation of the acetabular and femoral components on the range of motion of the hip
333 at different head-neck ratios. *J. Bone Joint Surg.-Am. Vol.* 82A, 315-321.

334 De Haan, R., Campbell, P.A., Su, E.P., De Smet, K.A., 2008a. Revision of metal-on-metal
335 resurfacing arthroplasty of the hip - The influence of malpositioning of the components. *J.*
336 *Bone Joint Surg.-Br. Vol.* 90B, 1158-1163.

337 De Haan, R., Pattyn, C., Gill, H.S., Murray, D.W., Campbell, P.A., De Smet, K., 2008b.
338 Correlation between inclination of the acetabular component and metal ion levels in metal-
339 on-metal hip resurfacing replacement. *J. Bone Joint Surg.-Br. Vol.* 90B, 1291-1297.

340 De Smet, K., De Haan, R., Calistri, A., Campbell, P.A., Ebrahimpour, E., Pattyn, C., Gill,
341 H.S., 2008a. Metal ion measurement as a diagnostic tool to identify problems with metal-on-
342 metal hip resurfacing. *Journal of Bone and Joint Surgery - Series A* 90, 202-208.

343 De Smet, K., De Haan, R., Calistri, A., Campbell, P.A., Ebrahimpour, E., Pattyn, C., Gill,
344 H.S., 2008b. Metal Ion Measurement as a Diagnostic Tool to Identify Problems with Metal-
345 on-Metal Hip Resurfacing.

346 Del Schutte, H., Lipman, A.J., Bannar, S.M., Livermore, J.T., Ilstrup, D., Morrey, B.F., 1998.
347 Effects of acetabular abduction on cup wear rates in total hip arthroplasty. *J. Arthroplast.* 13,
348 621-626.

349 Donell, S.T., Darrah, C., Nolan, J.F., Wimhurst, J., Toms, A., Barker, T.H.W., Case, C.P.,
350 Tucker, J.K., Group, N.M.-o.-M.S., 2010. Early failure of the Ultima metal-on-metal total hip
351 replacement in the presence of normal plain radiographs. *Journal of Bone & Joint Surgery,*
352 *British Volume* 92-B, 1501-1508.

353 Grammatopoulos, G., Langton, D., Kwon, Y.-M., Pandit, H., Gundle, R., McLardy-Smith, P.,
354 Whitwell, D., Murray, D., Gill, H., 2011. The role of acetabular component positioning in the
355 development of inflammatory pseudotumours. *J Bone Joint Surg Br* 93-B, 223-a-.

356 Grammatopoulos, G., Pandit, H., Glyn-Jones, S., McLardy-Smith, P., Gundle, R., Whitwell,
357 D., Gill, H.S., Murray, D.W., 2010. Optimal acetabular orientation for hip resurfacing.
358 Journal of Bone & Joint Surgery, British Volume 92-B, 1072-1078.

359 Gruen, T.A., Le Duff, M.J., Wisk, L.E., Amstutz, H.C., 2011. Prevalence and Clinical
360 Relevance of Radiographic Signs of Impingement in Metal-on-Metal Hybrid Hip
361 Resurfacing. The Journal of Bone & Joint Surgery 93, 1519-1526.

362 Kadaba, M.P., Ramakrishnan, H.K., Wootten, M.E., 1990. Measurement of lower extremity
363 kinematics during level walking. J. Orthop. Res. 8, 383-392.

364 Kennedy, J.G., Rogers, W.B., Soffe, K.E., Sullivan, R.J., Griffen, D.G., Sheehan, L.J., 1998.
365 Effect of acetabular component orientation on recurrent dislocation, pelvic osteolysis,
366 polyethylene wear, and component migration. The Journal of Arthroplasty 13, 530-534.

367 Klein Horsman, M.D., Koopman, H.F.J.M., van der Helm, F.C.T., Prosé, L.P., Veeger,
368 H.E.J., 2007. Morphological muscle and joint parameters for musculoskeletal modelling of
369 the lower extremity. Clinical Biomechanics 22, 239-247.

370 Kwon, Y.-M., Ostlere, S.J., McLardy-Smith, P., Athanasou, N.A., Gill, H.S., Murray, D.W.,
371 2011. "Asymptomatic" Pseudotumors After Metal-on-Metal Hip Resurfacing Arthroplasty:
372 Prevalence and Metal Ion Study. The Journal of Arthroplasty 26, 511-518.

373 Kwon, Y.M., Glyn-Jones, S., Simpson, D.J., Kamali, A., McLardy-Smith, P., Gill, H.S.,
374 Murray, D.W., *In vivo* wear analysis of metal-on-metal hip resurfacing implants revised due
375 to pseudotumours.

376 Kwon, Y.M., Glyn-Jones, S., Simpson, D.J., Kamali, A., McLardy-Smith, P., Gill, H.S.,
377 Murray, D.W., 2010. Analysis of wear of retrieved metal-on-metal hip resurfacing implants
378 revised due to pseudotumours. J. Bone Joint Surg.-Br. Vol. 92B, 356-361.

379 Kwon, Y.M., Ostlere, S., McLardy-Smith, P., Gundle, R., Whitwell, D., Gibbons, C.L.M.,
380 Athanasou, N., Gill, H.S., Murray, D.W., Year Metal ion levels in pseudotumours associated
381 with metal-on-metal hip resurfacings. In The 55th Orthopaedic Research Society Annual
382 Meeting. Las Vegas, USA.

383 Langton, D.J., Jameson, S.S., Joyce, T.J., Hallab, N.J., Natsu, S., Nargol, A.V.F., 2010. Early
384 failure of metal-on-metal bearings in hip resurfacing and large-diameter total hip
385 replacement. Journal of Bone & Joint Surgery, British Volume 92-B, 38-46.

386 Langton, D.J., Jameson, S.S., Joyce, T.J., Webb, J., Nargol, A.V.F., 2008. The effect of
387 component size and orientation on the concentrations of metal ions after resurfacing
388 arthroplasty of the hip. Journal of Bone & Joint Surgery, British Volume 90-B, 1143-1151.

389 Langton, D.J., Joyce, T.J., Jameson, S.S., Lord, J., Van Orsouw, M., Holland, J.P., Nargol,
390 A.V.F., De Smet, K.A., 2011. Adverse reaction to metal debris following hip resurfacing.
391 Journal of Bone & Joint Surgery, British Volume 93-B, 164-171.

392 Langton, D.J., Sprowson, A.P., Joyce, T.J., Reed, M., Carluke, I., Partington, P., Nargol,
393 A.V.F., 2009a. Blood metal ion concentrations after hip resurfacing arthroplasty: A
394 comparative study of articular surface replacement and Birmingham hip resurfacing
395 arthroplasties. *Journal of Bone and Joint Surgery - Series B* 91, 1287-1295.

396 Langton, D.J., Sprowson, A.P., Joyce, T.J., Reed, M., Carluke, I., Partington, P., Nargol,
397 A.V.F., 2009b. Blood metal ion concentrations after hip resurfacing arthroplasty: A
398 comparative study of articular surface replacement and Birmingham hip resurfacing
399 arthroplasties. *J. Bone Joint Surg.-Br. Vol.* 91B, 1287-1295.

400 Le Duff, M., Johnson, A., Wassef, A., Amstutz, H., 2014. Does Femoral Neck to Cup
401 Impingement Affect Metal Ion Levels in Hip Resurfacing? *Clin Orthop Relat Res* 472, 489-
402 496.

403 Lewinnek, G.E., Lewis, J.L., Tarr, R., Compere, C.L., Zimmerman, J.R., 1978a. Dislocations
404 after total hip-replacement arthroplasties. *The Journal of Bone & Joint Surgery* 60, 217-220.

405 Lewinnek, G.E., Lewis, J.L., Tarr, R., Compere, C.L., Zimmerman, J.R., 1978b. Dislocations
406 after total hip-replacement arthroplasties. *J. Bone Joint Surg.-Am. Vol.* 60, 217-220.

407 Lim, S.-J., Kim, J.-H., Moon, Y.-W., Park, Y.-S., 2012. Femoroacetabular Cup Impingement
408 After Resurfacing Arthroplasty of the Hip. *The Journal of Arthroplasty* 27, 60-65.

409 Lund, M.E.A., M. S.; de Zee, M; Rasmussen, J, Year Functional Scaling of Musculoskeletal
410 Models. In XXIIIrd Congress of the International Society of Biomechanics. Brussels,
411 Belgium.

412 Matthies, A.K., Henckel, J., Cro, S., Suarez, A., Noble, P.C., Skinner, J., Hart, A.J., 2014.
413 Predicting wear and blood metal ion levels in metal-on-metal hip resurfacing. *J. Orthop. Res.*
414 32, 167-174.

415 Matthies, A.K., Skinner, J.A., Osmani, H., Henckel, J., Hart, A.J., 2012. Pseudotumors Are
416 Common in Well-positioned Low-wearing Metal-on-Metal Hips. *Clinical orthopaedics and*
417 *related research* 470, 1895-1906.

418 Mellon, S.J., Grammatopoulos, G., Andersen, M.S., Pegg, E.C., Pandit, H.G., Murray, D.W.,
419 Gill, H.S., 2013. Individual motion patterns during gait and sit-to-stand contribute to edge-
420 loading risk in metal-on-metal hip resurfacing. *Proceedings of the Institution of Mechanical*
421 *Engineers, Part H: Journal of Engineering in Medicine* 227, 799-810.

422 Pandit, H., Glyn-Jones, S., McLardy-Smith, P., Gundle, R., Whitwell, D., Gibbons, C.L.M.,
423 Ostlere, S., Athanasou, N., Gill, H.S., Murray, D.W., 2008a. Pseudotumours associated with
424 metal-on-metal hip resurfacings. *Journal of Bone and Joint Surgery - Series B* 90, 847-851.

425 Pandit, H., Vlychou, M., Whitwell, D., Crook, D., Luqmani, R., Ostlere, S., Murray, D.,
426 Athanasou, N., 2008b. Necrotic granulomatous pseudotumours in bilateral resurfacing hip
427 arthroplasties: evidence for a type IV immune response. *Virchows Archiv* 453, 529-534.

- 428 Schmalzried, T.P., 2009. Metal-metal bearing surfaces in hip arthroplasty. *Orthopedics* 32.
- 429 van Arkel, R.J., Modenese, L., Phillips, A.T.M., Jeffers, J.R.T., 2013. Hip abduction can
430 prevent posterior edge loading of hip replacements. *J. Orthop. Res.* 31, 1172-1179.
- 431 Wiadrowski, T.P., McGee, M., Cornish, B.L., Howie, D.W., 1991. Peripheral wear of
432 Wagner resurfacing hip arthroplasty acetabular components. *The Journal of Arthroplasty* 6,
433 103-107.
- 434 Widmer, K.H., Zurfluh, B., 2004. Compliant positioning of total hip components for optimal
435 range of motion. *Journal of Orthopaedic Research* 22, 815-821.
- 436 Willert, H.-G., Buchhorn, G.H., Dipl, I., Fayyazi, A., Flury, R., Windler, M., Köster, G.,
437 Lohmann, C.H., 2005. Metal-on-Metal Bearings and Hypersensitivity in Patients with
438 Artificial Hip Joints A Clinical and Histomorphological Study. *The Journal of Bone & Joint*
439 *Surgery* 87, 28-36.
- 440 Yoo, M.C., Cho, Y.J., Chun, Y.S., Rhyu, K.H., 2011. Impingement Between the Acetabular
441 Cup and the Femoral Neck After Hip Resurfacing Arthroplasty. *The Journal of Bone & Joint*
442 *Surgery* 93, 99-106.
- 443 Yoon, J., Le Duff, M., Johnson, A., Takamura, K., Ebrahimzadeh, E., Amstutz, H., 2013.
444 Contact patch to rim distance predicts metal ion levels in hip resurfacing. *Clinical*
445 *orthopaedics and related research* 471, 1615-1621.

446
447 Tables

448 *Table 1. Subject information*

Subject	Gender	Implant/ head dia. (mm)	Radiographic Inclination/ Anteversion (°)	Serum Chromium level (µg/l)	Serum Cobalt level (µg/l)	Optimum Inclination/ Anteversion (°)	Total Angle (°) Change Actual-to Optimal
1	F	BHR/52	52/20	3.2	2.6	38/24	14.6
2	F	CON/48	43/14	2.4	1.6	34/26	15.0
3	M	CON/50	46/23	0.5	0.8	48/7	16.1
4	M	BHR/54	49/14	1.8	1.3	47/7	7.3
5	F	CON/44	44/19	0.6	0.7	26/-1	26.9
6	M	BHR/58	48/18	0.7	1.2	33/15	15.3
7	M	CON/48	62/10	2	3.6	34/26	32.3
8	M	BHR/50	38/33	0.5	1	41/21	12.4
9	F	CON/46	43/4	1.3	1.6	38/1	5.8
10	F	BHR/54	65/8	4.4	2.1	45/6	20.1
11	M	BHR/50	61/1	1.4	1.4	41/21	28.3
12	M	CON/54	56/13	1.3	2.4	37/20	20.2
13	M	CON/50	56/34	6.1	3.1	38/14	26.9
14	M	CON/52	35/-10	5.8	4.7	42/20	30.8
15	F	BHR/38	60/14	7.8	4.6	40/23	21.9
16	F	BHR/46	60/8	6.8	9.3	53/8	7.0

Figures

Figure 1. Risk of impingement was calculated using an ellipse fitted to points around the femoral neck in the XY plane of the coordinate system local to the femoral component. The position of this ellipse relative to the cup edge was determined for four activities of daily living. Impingement was defined as the positions of the cup edge and the ellipse overlapping.

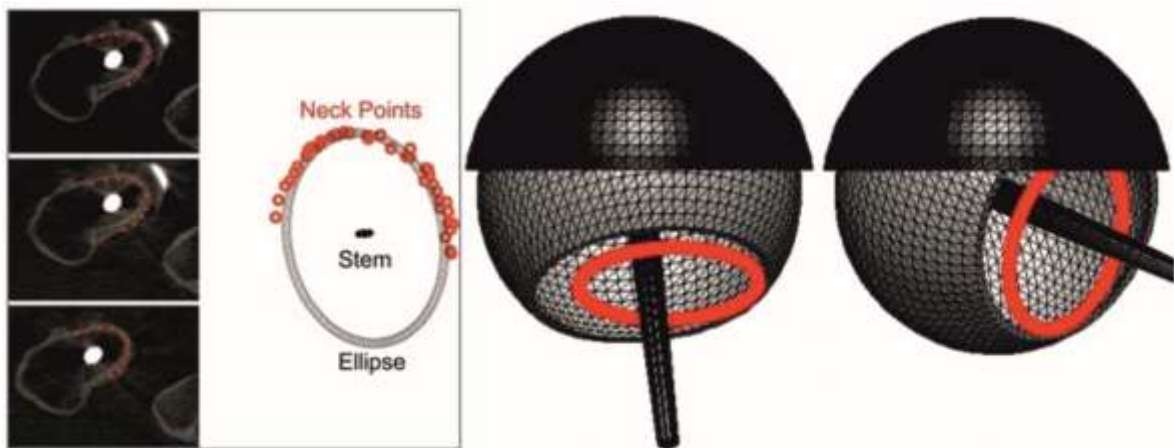
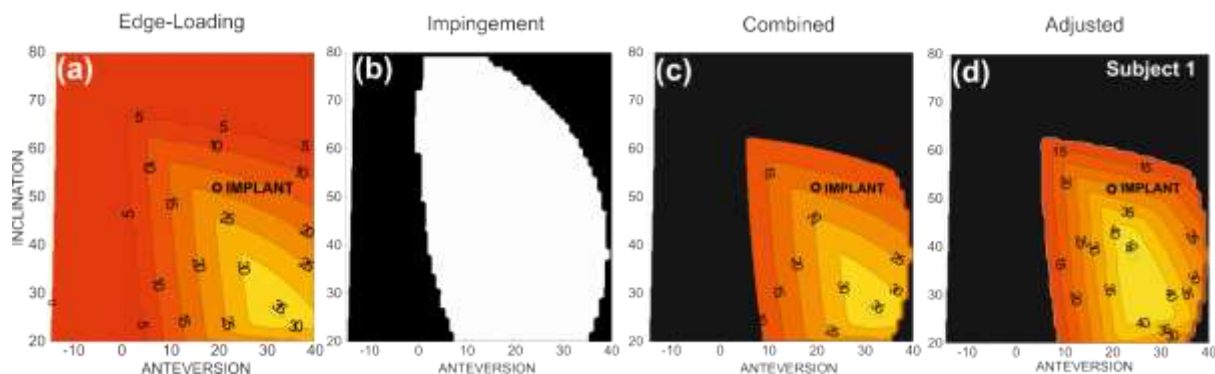
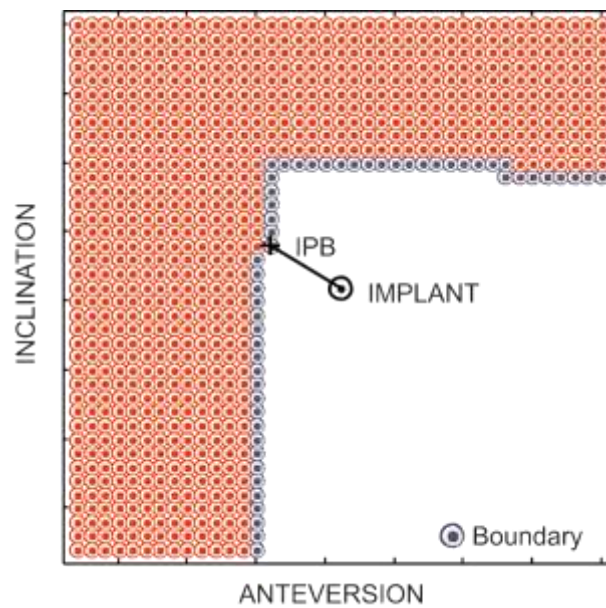


Figure 2. (a) Edge-loading, (b) Impingement, (c) Combined and (d) Adjusted plots for Subject 1. Numbers within Edge-loading and Combined plots represent the %CPR distance. In the impingement plot the white area represents orientations free from impingement for the activities analysed. In the combined plot the 'safe' zone are orientations free from impingement and edge-loading (CPR distance < 10%). In the adjusted plot, the distance from the safe zone boundary has been added to the %CPR in order to define the optimal orientation (38/24 Inclination/Anteversion)



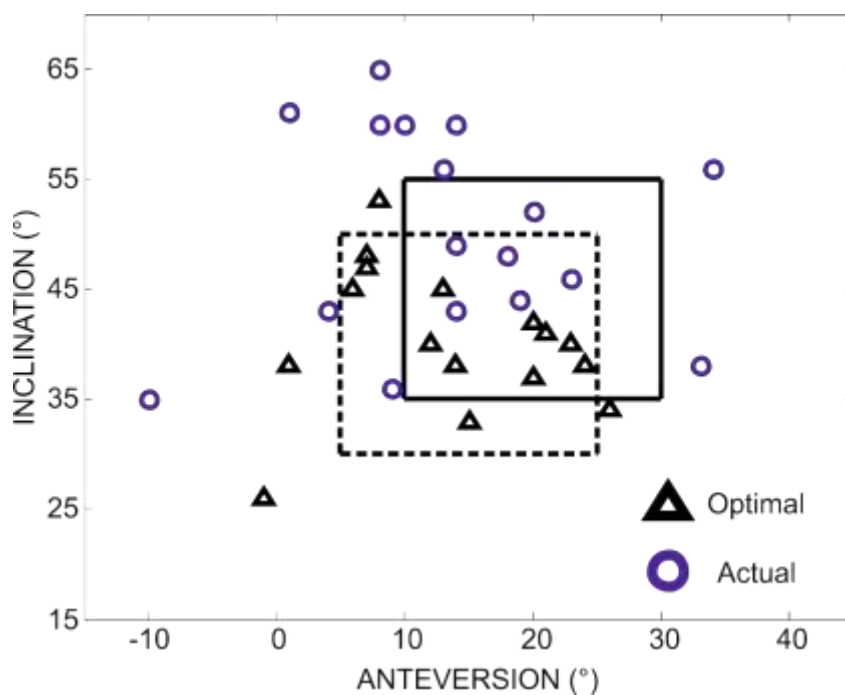
464 Figure 3. Implant Position to Boundary (IPB) was calculated as the smallest distance from the
 465 subjects' actual implant orientation to the boundary of the safe zone



466

467

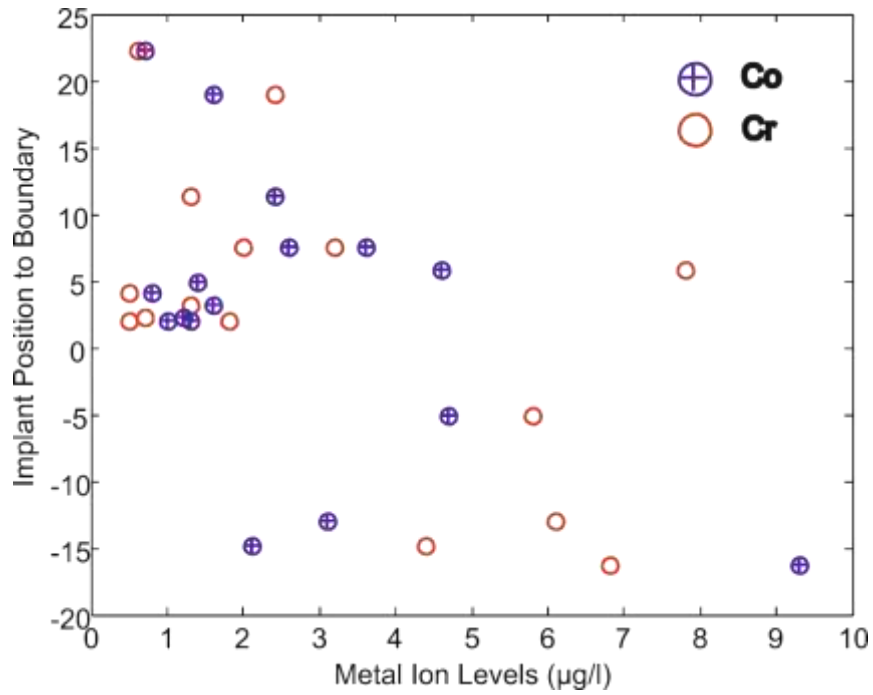
468 Figure 4. Actual and optimal orientations for 16 Subjects with MoMHRA. Box with solid
 469 sides represents a zone with reduced risk of pseudotumour(Grammatopoulos et al., 2010). Box
 470 with dashed sides represents a zone with reduced risk of dislocation in THR(Lewinnek et al.,
 471 1978a)



472

473

474 Figure 5. Implant Position to Boundary (IPB) versus serum cobalt and chromium. There was
475 a statistically significant correlation between IPB and serum chromium ($p = 0.01$) and serum
476 cobalt ($p = 0.016$) ions.



477

478

479

480